

Systematics of intrinsic oxygen fugacity–temperature relationships in multi-phase assemblages

STEPHEN E. DELONG

Department of Geological Sciences
State University of New York at Albany
Albany, New York 12222

Abstract

If multiple phases of an assemblage closed to oxygen exchange at a particular oxygen fugacity and temperature, their curves on a plot of $\log f(\text{O}_2)$ vs. $1/T$ should ideally intersect at a common point defining the conditions of equilibrium. Measured curves will show some experimental scatter, however, so that an assemblage of n phases may define up to $(n/2)(n - 1)$ intersections. The ambiguity inherent in estimating the equilibrium $\log f(\text{O}_2)$ (L_E) and temperature (T_E) from this scatter can be avoided by use of a plot based on the following equation:

$$L_0 = (1/T_0 - 1/T_E)H + L_E$$

where H is the slope of each experimental curve, T_0 is an arbitrary reference temperature, and L_0 is the value of $\log f(\text{O}_2)$ for each curve at $1/T_0$. Thus, on a plot of L_0 vs. H , the curve for each phase is transformed to a point, and a mutually equilibrated assemblage defines a straight line (an isotherm) with slope and intercept proportional to T_E and L_E , respectively. Application of this procedure to published data for the Oka carbonatite and the Bushveld complex shows the value of this approach in providing a statistical test for mutual equilibration of a multi-phase assemblage. This type of plot may also be useful in recognizing more complex redox situations, including open-system re-equilibration.

Introduction

Most applications of the double-cell zirconia electrolyte technique (Sato, 1971, 1972) for measuring intrinsic oxygen fugacity, $f(\text{O}_2)$, have been restricted to inferences of relative oxidation states, e.g., that type A spinel peridotites are more reduced than type B peridotites and megacryst ilmenites (Arculus et al., 1984; see also Arculus and Delano, 1981, and Haggerty and Tompkins, 1983). As Sato (1971) originally suggested, however, another potentially valuable facet of the technique is as a geothermometer and oxygen geobarometer. This suggestion is based on the assumption that all phases of a rock closed with respect to oxygen exchange at the same values of T and $f(\text{O}_2)$. Therefore, experimentally determined curves of $\log f(\text{O}_2)$ vs. $1/T$ for two or more phases from such a rock should intersect at the point of final equilibration (Sato, 1971, Fig. 14, p. 87).

Sato (1972) first demonstrated an application of this procedure with co-existing olivine and chromite from a chromitite layer in the Stillwater Complex. Curves for these two phases yielded a temperature that was compatible with independent estimates for other layers from the same horizon. Despite the promise of this technique, there are only two successful applications of it to multi-phase assemblages for which detailed measurements have been published—the Oka carbonatite (Friel and Ulmer, 1974) and the Critical Zone of the Bushveld Complex (Flynn et al., 1978). In the balance of this paper, I discuss two topics that amplify or extend the technique suggested by Sato. First, I describe an alternative scheme for estimating T and $f(\text{O}_2)$ of equi-

libration for multi-phase assemblages that is more amenable to conventional statistical treatment and illustrate its application with the Oka and Bushveld data. Second, I discuss from a qualitative perspective the kind of information that might be accessible from assemblages in which more complex redox behavior has occurred.

Estimating T and $f(\text{O}_2)$

The traditional format for presentation of $f(\text{O}_2)$ data is the thermodynamically-based plot of $\log f(\text{O}_2)$ vs. $1/T$ (reciprocal absolute temperature). For a buffer reaction involving simple, pure phases (e.g., $\text{Ni} + 1/2 \text{O}_2 = \text{NiO}$), the slope of such a plot is proportional to the standard enthalpy of the reaction, ΔH° , through the common variant of the van't Hoff equation,

$$\frac{d \ln K}{d(1/T)} = - \frac{\Delta H^\circ}{R},$$

where R is the gas constant and K the equilibrium constant. The activities of pure solid phases are unity, so that $\ln K$ can be replaced by $\ln f(\text{O}_2)$ (or, equivalently, $2.303 \log f(\text{O}_2)$). An analogous thermodynamic interpretation is presumably appropriate for a curve defined experimentally for a natural single phase (see Sato, 1972), though the reaction mechanism is internal defect exchange rather than buffering (Flood and Hill, 1957). In order to emphasize the distinction between these reaction mechanisms, I use the modifiers "buffer" and "index" (= internal defect exchange) as appropriate. (For readers who are etymological buffs, it is

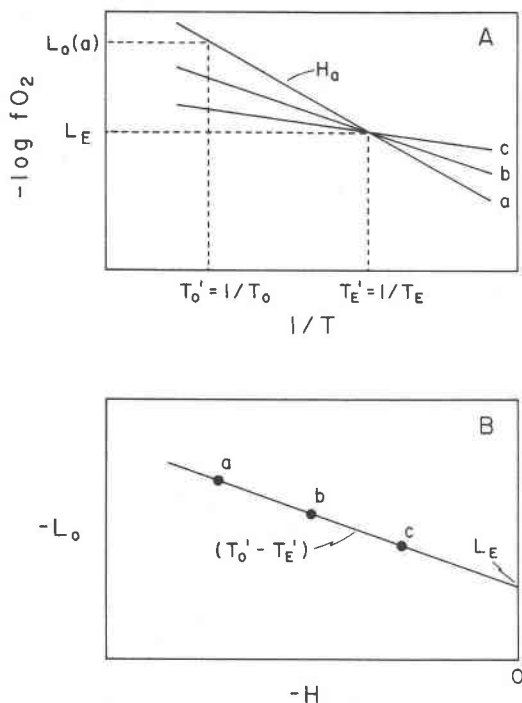


Fig. 1. (A) Standard $\log f(\text{O}_2)$ vs. $1/T$ plot of internal defect exchange (= index) curves of slope H for three phases (a, b, c) equilibrated at some temperature, T_E , and $\log f(\text{O}_2)$, L_E . T_0 is the reference temperature at which the $\log f(\text{O}_2)$ value, L_0 , is determined for each phase. (B) $f(\text{O}_2)$ isotherm plot, where the index curve for each phase in A is transformed (see equation 2) to a point. The slope of this line is proportional to T_E and the intercept on the L_0 axis is L_E .

worth noting that one of the definitions of "index" in Webster's New World Dictionary is "indication; sign; representation," as in: a curve of $\log f(\text{O}_2)$ vs. $1/T$ is an *index* of intrinsic oxidation state.)

In an assemblage that closed to oxygen exchange at a particular temperature, the several phases (whose index reactions are assumed to have different values of ΔH°) should define different index curves that have a common intersection point, $(1/T, \log f(\text{O}_2))$, at which the assemblage last equilibrated. This situation is illustrated schematically in Figure 1A for an assemblage of three phases (a, b, c), where the notation has been simplified somewhat so that $(T'_E, L_E) = (1/T, \log f(\text{O}_2))_{\text{equil}}$. Each of these index curves can be described by a line in point-slope form:

$$\frac{L_0 - L_E}{1/T_0 - 1/T_E} = \frac{L_0 - L_E}{T'_0 - T'_E} = \frac{-\Delta H^\circ}{2.303R} = H, \quad (1)$$

where T_0 is some fixed reference temperature and L_0 is the value of $\log f(\text{O}_2)$ for the phase at that temperature. Because of possible variation of ΔH° over a large range of temperature, it would be preferable to choose T_0 so that it is within or near the experimentally accessible limits, though that choice is not required mathematically.

A simple rearrangement of equation (1) then yields

$$L_0 = (T'_0 - T'_E)H + L_E, \quad (2)$$

which transforms the experimental index curves (Fig. 1A) into a linear plot of L_0 vs. H (see Figure 1B). The slope of this line is a function only of T'_0 and T'_E and hence the line is an isotherm; the intercept is L_E , so that the equilibrium temperature (T_E) and $\log f(\text{O}_2)$ (L_E) can be determined directly from a least-squares fit.

Applications

The results for Oka and Bushveld discussed below are based on the data reported by Ulmer and colleagues. For each phase, I have recalculated the experimental index curve using the least-squares cubic formulation of York (1966; see also Brooks et al., 1972), which allows for an estimate of the correlation (r) between the errors in T and $\log f(\text{O}_2)$. In all cases reported here, I have chosen a value of 0.9 for r because of the theoretical expectation and experimental demonstration of strong dependence of measured $\log f(\text{O}_2)$ on $1/T$ (e.g., Arculus and Delano, 1981). The reference temperature, T_0 , at which the values of L_0 were calculated for each curve, was chosen so that $1/T_0 = 7 \times 10^{-4} \text{K}^{-1}$ ($T_0 \cong 1155^\circ\text{C}$). Error estimates for $1/T - 1/T_0$ ranged from $\pm 20 \times 10^{-6} \text{K}^{-1}$ at 600°C to $\pm 1 \times 10^{-6} \text{K}^{-1}$ at 1100°C , based on the uncertainties reported by Friel and Ulmer (1974, Table 1, p. 315). Error estimates for experimental values of $\log f(\text{O}_2)$ ranged from ± 0.5 at 600°C to ± 0.2 at 1100°C , based on (or extrapolated from) the uncertainties reported by Flynn et al. (1978, p. 144; note that those uncertainties are in log units, not atm).

Oka carbonatite

Friel and Ulmer (1974) determined $f(\text{O}_2)$ over the temperature range $600\text{--}1000^\circ\text{C}$ for three coexisting phases from the Oka carbonatite: olivine, magnetite, and lattrapite (a Nb-rich perovskite). Taken in pairs, the three index curves defined intersections ranging from about 680 to 740°C . These points in turn defined what Friel and Ulmer (1974, p. 315) termed a "triangle of uncertainty in the intersection of the three curves," which was centered at $710 \pm 15^\circ\text{C}$ and $\log f(\text{O}_2) = -17.1 \pm 0.5$. They also showed that these values were generally compatible with independent estimates (e.g., from carbon and oxygen isotope equilibria for calcite and magnetite) of physical conditions during crystallization of the Oka body and interpreted the center of the triangle of intersection as indicating mutual equilibration of the three phases at that T and $f(\text{O}_2)$.

Table 1 gives (a) the values of H and L_0 derived from a least-squares fit of equation (1) to Friel and Ulmer's data for each of the Oka phases and (b) the results of fitting a single line for equation (2) to the values derived in (a). The latter results are shown graphically in Figure 2. First, it is clear from this diagram that all three phases fall on a single line within the calculated uncertainties in H and L_0 and therefore that the interpretation of a common T and $f(\text{O}_2)$ of equilibrium is statistically reasonable. Second, the specific values of $T_E = 725 + 77/-67^\circ\text{C}$ and $L_E = -16.56 \pm 1.95$

Table 1. Calculated intrinsic $f(\text{O}_2)$ - T parameters for Oka carbonatite*

Sample (# pts.)	H (= slope)	L_0 (= intercept)
Olivine (6)	- 14,031 ± 1,447	- 12.40 ± 0.39
Magnetite (6)	- 16,416 ± 1,944	- 11.43 ± 0.46
Latrappite (9)	- 24,302 ± 1,322	- 9.24 ± 0.30
Combined assemblage - L_0 vs. H (eq. 2):		
$1/T_0 - 1/T_E = \text{slope} = - (3.021 \pm 0.717) \times 10^{-4}$		
$T_E = 725 \begin{smallmatrix} +77 \\ -67 \end{smallmatrix} \text{ } ^\circ\text{C}$		
$L_E = \text{intercept} = -16.56 \pm 1.95$		
Reference temperature chosen so that $1/T_0 = 7 \times 10^{-4}$		
* Original data from Friel and Ulmer (1974).		

log units agree well with Friel and Ulmer's estimates, though my uncertainties are considerably larger than Friel and Ulmer's (see previous paragraph). This discrepancy is not surprising, because their uncertainties were apparently only visual estimates. The large magnitude of the uncertainty in L_E is understandable because of the extrapolation required to reach the intercept from the most reduced point (olivine—see Fig. 2) and because of the relatively large error limits on L_0 for each of the three phases (compare with errors for L_0 in Figure 3 below).

Bushveld Complex

Flynn et al. (1978) determined $f(\text{O}_2)$ over the temperature range 800–1100°C for several samples at and immediately above the contact of the E- and F-horizons of the Critical Zone of the Bushveld Complex. The samples, taken over a vertical distance of about 2 cm, included chromite from a chromitite layer at the contact and overlying whole-rock anorthosite, whole-rock pyroxenite, and separated plagioclase and bronzite from the respective whole rocks.

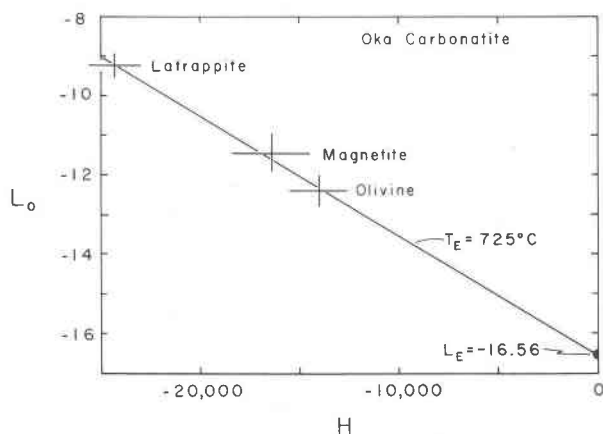


Fig. 2. $f(\text{O}_2)$ isotherm plot for phases from the Oka carbonatite (Friel and Ulmer, 1974). H is the slope of the index curve for each phase on the $\log f(\text{O}_2)$ vs. $1/T$ plot, and L_0 is the value of $\log f(\text{O}_2)$ on that curve corresponding to $1/T_0$.

Table 2. Calculated intrinsic $f(\text{O}_2)$ - T parameters for Bushveld Complex*

Sample (# pts.)	H (= slope)	L_0 (= intercept)
Bronzite (4)	- 10,915 ± 4,454	- 11.91 ± 0.82
Anorthosite (14)	- 11,994 ± 1,185	- 11.23 ± 0.14
Plagioclase (14)	- 14,487 ± 1,205	- 11.37 ± 0.15
Pyroxenite (14)	- 16,429 ± 1,218	- 11.28 ± 0.15
Chromite (14)	- 24,849 ± 1,231	- 11.00 ± 0.15
Combined assemblage - L_0 vs. H (eq. 2):		
$1/T_0 - 1/T_E = \text{slope} = - (2.619 \pm 1.608) \times 10^{-5}$		
$T_E = 1104 \begin{smallmatrix} +31 \\ -30 \end{smallmatrix} \text{ } ^\circ\text{C}$		
$L_E = \text{intercept} = -11.67 \pm 0.32$		
Reference temperature chosen so that $1/T_0 = 7 \times 10^{-4}$		
* Original data from Flynn et al. (1978).		

The index curves for these five samples yielded eight intersections, of which Flynn et al. considered only those involving the chromite curve: (1) chromite-anorthosite, 1127°C, $\log f(\text{O}_2) = -11.38$; (2) chromite-pyroxenite-plagioclase, 1091°C, -11.82 ; and (3) chromite-bronzite, 1055°C, -12.30 . Coincidentally, the average for all three was equal to that for the triple intersection, and Flynn et al. (1978, p. 146) concluded that the conditions of equilibration for all five samples were best given by $1091 \pm 35^\circ\text{C}$ and $\log f(\text{O}_2) = -11.82 \pm 0.4$. This conclusion is somewhat obscured, however, by the caption of their Figure 9 (Flynn et al., 1978, p. 149) in which they suggested that each of the three intersections listed above represented a separate "last equilibration" of chromite with the other samples (see also, Ulmer et al., 1976, p. 657).

Table 2 gives the results of recalculating the Bushveld data to fit equations (1) and (2), and the latter are shown in Figure 3. As the graph indicates, all points fall on the same isotherm, so that within the error limits it is reasonable to consider that the five samples equilibrated under common conditions, and conversely it is unreasonable to consider that different mutual intersections of these particular index

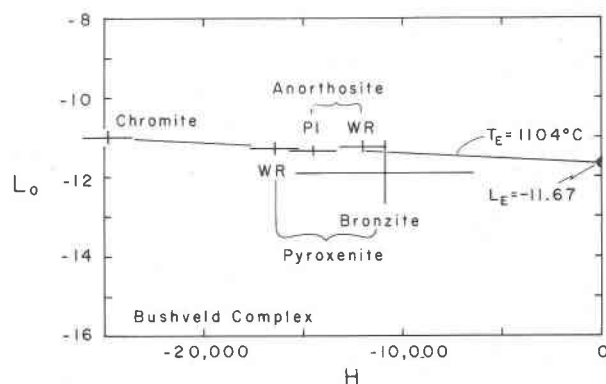


Fig. 3. $f(\text{O}_2)$ isotherm plot for phases from the Bushveld Complex (Flynn et al., 1978). (See Fig. 2 for explanation of H and L_0 .)

curves have any physical meaning. The resulting values of $T_E = 1104 + 31/-30^\circ\text{C}$ and $L_E = -11.67 \pm 0.32$ log units agree well with the estimates of Flynn et al. Omitting the point for the bronzite sample (which has very large uncertainties) makes a negligible difference in these values.

Discussion and extensions

As illustrated by the Bushveld data (Flynn et al., Fig. 9, p. 149), there may be considerable ambiguity in trying to infer T_E and L_E from intersections of multiple index curves. More generally, the experimental scatter in measured curves for n phases can yield up to $(n/2)(n-1)$ intersections, even though the phases were mutually equilibrated. The approach used in this paper avoids this dilemma, because the transformation scheme based on equation (2) is amenable to more conventional statistical error analysis. York's (1966) least-squares cubic formulation is particularly convenient in this regard because, as noted above, it allows for the strong correlation between errors in measurement of T and $\log f(\text{O}_2)$, thereby providing uncertainties in H and L_0 for each phase. Use of the values of H and L_0 and their resultant uncertainties in a second application of York's formulation to calculate T_E and L_E for the suite is in no way logically circular, although it is possible that there could be subtle error propagation effects that might influence the calculated uncertainties in T_E and L_E in particular. In the absence of additional published experimental data, this question remains open to speculation.

Regardless of the details of how the statistics are handled, the advantage in principle of the approach described here for calculating T_E and L_E is that it is immediately possible to determine whether the index curve for a particular phase—and its transformation through equation (2) to a point on the $f(\text{O}_2)$ isotherm plot—provides evidence that it was in equilibrium with the other phases or whether a more complex redox history may be indicated. For two cases where high-quality, multi-phase data are available in the literature (i.e., Oka and Bushveld), the interpretation of simple equilibrium appears to be adequate.

This argument, and indeed the entire idea developed in this paper, has an obvious parallel in the advantage of the strontium isochron plot ($^{87}\text{Sr}/^{86}\text{Sr}$ vs. $^{87}\text{Rb}/^{86}\text{Sr}$) over the strontium evolution diagram ($^{87}\text{Sr}/^{86}\text{Sr}$ vs. time) as used in geochronology. (Readers unfamiliar with Rb-Sr systematics are referred to Faure (1977), who gives examples of these plots and the other isotopic relationships discussed below.) At the risk of extending that analogy beyond its useful limits, it is worth asking whether any of the other aspects of the strontium isochron plot might provide additional insight into the interpretation of intrinsic $f(\text{O}_2)$ data.

For example, what would be the redox analog to the internal re-distribution of Rb/Sr and re-equilibration of $^{87}\text{Sr}/^{86}\text{Sr}$ during metamorphism, which ideally yields a whole-rock isochron defining an original age and a flatter mineral isochron indicating the time of subsequent disturbance? A comparable situation for intrinsic $f(\text{O}_2)$ would be one in which a geological system that had originally equi-

librated at T_E and L_E underwent an internal redox re-equilibration at a different temperature, T_{E^*} , that resulted in no net gain or loss of oxygen (i.e., $L_{E^*} = L_E$). This case is illustrated schematically in Figure 4 for three nominal whole-rock samples and two of their constituent minerals that underwent re-equilibration at the same $\log f(\text{O}_2)$ but a lower temperature, $T_{E^*} < T_E$. There are geologically important reactions that could satisfy the formal requirements of this case when taken in isolation (e.g., hematite + ulvöspinel = magnetite + ilmenite), although it is questionable whether they would occur naturally under truly isochemical conditions. The significant point in the present context, however, is that the ambiguity of multiple intersections of index curves in Figure 4A is eliminated by the transformation to Figure 4B. Thus, such a situation could be recognized in the seemingly unlikely event that an appropriate natural occurrence was studied experimentally.

As a second and presumably more realistic example, Figure 5 presents hypothetical results for an open-system case. Figures 5A and 5B show the standard index-curve diagram and the $f(\text{O}_2)$ isotherm plot, respectively, for the constituent minerals of two whole-rock samples (M, N) from an igneous or metamorphic body that originally equilibrated at T_E , L_E . Imagine that N undergoes re-equilibration at a lower temperature, $T_{E^*} < T_E$, and more reduced conditions, $L_{E^*} < L_E$, but M remains unchanged. Such a situation might arise, for example, if N is near the contact with a later intrusion but M is sufficiently distant

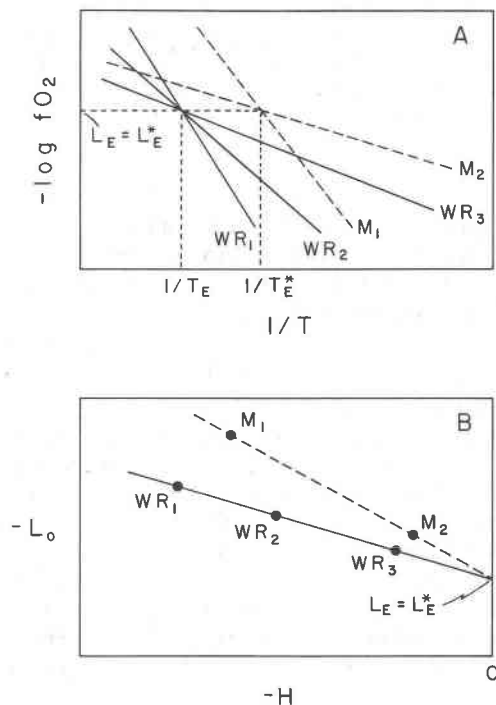


Fig. 4. Isochemical re-equilibration at $T_{E^*} < T_E$ and $L_{E^*} = L_E$ of minerals (M_1 , M_2) from whole-rock samples (WR₁, WR₂, WR₃) that originally equilibrated at T_E , L_E . (A) Index-curve plot. (B) $f(\text{O}_2)$ isotherm plot.

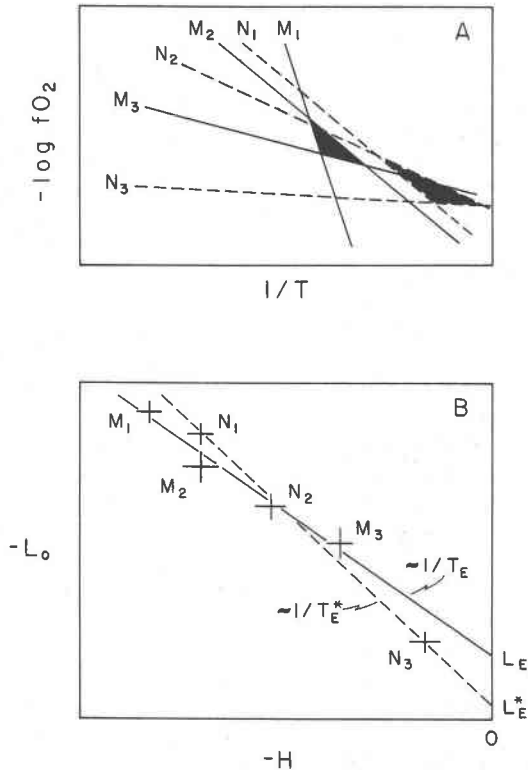


Fig. 5. (A) Index-curve plot for three constituent minerals (M_1, M_2, M_3) from whole-rock sample M equilibrated at T_E, L_E (solid lines) and for three minerals (N_1, N_2, N_3) from whole-rock N that re-equilibrated at T_{E^*}, L_{E^*} (dashed lines). Stippled areas show triangles of intersection for the T, L pairs that might be defined by real experimental data for each assemblage. (B) $f(O_2)$ isotherm plot for A with simulated experimental uncertainties.

that its redox state is unaffected. The resulting welter of intersecting index curves (Fig. 5A) might not clearly reveal this scenario, but the $f(O_2)$ isotherm plot could more readily do so (Fig. 5B). Similar cases can be devised for other open-system conditions (e.g., $T_{E^*} < T_E, L_{E^*} > L_E$).

Conclusion

In the absence of additional experimental data, it is not possible to assess fully the value of the analogy between the strontium isochron plot and the $f(O_2)$ isotherm plot nor the value of the hypothetical extensions of the latter to more complex redox situations. Perhaps the availability of the scheme will provide more motivation to explore such applications. One obviously fruitful area would be straightforward geothermometry/oxygen geobarometry of simple igneous and metamorphic systems, as I have tried to demonstrate here using the data from the Oka carbonatite and

the Bushveld Complex. A more ambitious effort, but one that could yield more fundamental insights, would be to examine open-system cases as a means of constraining the scale of oxygen exchange during natural redox processes, which would complement laboratory investigations of oxygen diffusion in simpler systems.

Acknowledgments

I thank K. E. Davis, J. W. Delano, T. M. Harrison, D. Loureiro, and G. W. Putman for discussion of the ideas presented here; T. M. Harrison for use of his implementation of York's least-squares cubic program; and R. J. Arculus, K. E. Davis, G. C. Ulmer, and E. B. Watson for comments on the manuscript.

References

- Arculus, R. J., Dawson, J. B., Mitchell, R. H., Gust, D. A., and Holmes, R. D. (1984) Oxidation states of the upper mantle recorded by megacryst ilmenite in kimberlite and type A and B spinel lherzolites. *Contributions to Mineralogy and Petrology*, 85, 85–94.
- Arculus, R. J. and Delano, J. W. (1981) Intrinsic oxygen fugacity measurements: Techniques and results for spinels from upper mantle peridotite and megacryst assemblages. *Geochimica et Cosmochimica Acta*, 45, 899–913.
- Brooks, C., Hart, S. R., and Wendt, I. (1972) Realistic use of two-error regression treatments as applied to rubidium-strontium data. *Reviews of Geophysics and Space Physics*, 10, 551–577.
- Faure, G. (1977) *Principles of Isotope Geology*. John Wiley and Sons, New York.
- Flood, H. and Hill, D. G. (1957) The redox equilibrium in iron oxide spinels and related systems. *Zeitschrift für Elektrochemie*, 61, 18–24.
- Flynn, R. T., Ulmer, G. C., and Sutphen, C. F. (1978) Petrogenesis of the eastern Bushveld Complex: Crystallization of the middle Critical Zone. *Journal of Petrology*, 19, 136–152.
- Friel, J. J. and Ulmer, G. C. (1974) Oxygen fugacity geothermometry of the Oka carbonatite. *American Mineralogist*, 59, 314–318.
- Haggerty, S. E. and Tompkins, L. A. (1983) Redox state of earth's upper mantle from kimberlitic ilmenites. *Nature*, 303, 295–300.
- Sato, M. (1971) Electrochemical measurements and control of oxygen fugacity and other gaseous fugacities with solid electrolyte sensors. In G. C. Ulmer, Ed., *Research Techniques for High Pressure and High Temperature*, p. 43–99. Springer-Verlag, New York.
- Sato, M. (1972) Intrinsic oxygen fugacities of iron-bearing oxide and silicate minerals under low total pressure. *Geological Society of America Memoir* 135, 289–307.
- Ulmer, G. C., Rosenhauer, M., Woermann, E., Ginder, J., Drory-Wolff, A., and Wasilewski, P. (1976) Applicability of electrochemical oxygen fugacity measurements to geothermometry. *American Mineralogist*, 61, 653–660.
- York, D. (1966) Least-squares fitting of a straight line. *Canadian Journal of Physics*, 44, 1079–1086.

Manuscript received, December 12, 1984;
accepted for publication, July 1, 1985.